Measurement of surface-plasmon dispersion in oxidized aluminum films*

R. B. Pettit,† J. Silcox, and R. Vincent
School of Applied and Engineering Physics, Cornell University, Ithaca, New York 14850
(Received 19 December 1973; revised manuscript received 25 November 1974)

A 75-keV electron beam with a low angular divergence (8×10^{-6} rad) combined with a Wien filter spectrometer is used to measure the dispersion of the ω^+ and ω^- modes for suface plasmons in thin oxidized aluminum films. The results for normal incidence and for tilted films are self-consistent and are also in reasonable agreement with theoretical curves calculated for a 35- to 40-Å oxide layer, provided reasonable assumptions are made about the composition and dielectric constants of the aluminum oxide.

I. INTRODUCTION

Several methods have been used to measure the dispersion of surface plasmons in metals. In the short-wavelength limit, low-energy-electron diffraction experiments[1] have detected deviations from the asymptotic energy, $\hbar\omega_s$, predicted by the local approximation for the dielectric constant. For long wavelengths the dispersion differs from the original equations derived by Ritchie[2,3] due to the retardation of the electromagnetic fields[4-6]; the dispersion curves are constrained to lie below the light line, $\omega = ck_s$, where $\hbar k_s$, the momentum vector of the surface plasmon, lies in the plane of the film. In films less than 300 Å thick, the two solutions for the Maxwell equations describing the fields can be resolved into separate curves [$\omega^+(k_s)$ and $\omega^-(k_s)$] with different excitation probabilities. We report here electron spectrometry measurements of the surface-plasmon dispersion relation in aluminum spanning the energy range from 2 to 11 eV, which extends from the short-wavelength limit (large k_s) where $\omega \simeq \omega_s$ all the way to the long-wavelength limit (small k_s) where $\omega \simeq ck_s$.

In principle, optical techniques[7,8] are the most accurate method for investigating the surface-plasmon dispersion. The measurements of Cowan and Arakawa[9,10] on absorption anomalies in p-polarized light diffracted from a concave grating coated with multilayer aluminum plus dielectric films are in good agreement with theory. However, their data are restricted to photon energies between 1.5 and 4.0 eV, and no peaks attributable to the ω^+ mode were observed in this energy range.

An alternative approach is to measure the energy and momentum change for high-energy electrons transmitted through the film. Ideally, a highly collimated source of monochromatic electrons, coupled to a spectrometer with approximately 0.1-eV resolution, is required to resolve typical plasmon half-widths of 0.5 eV.[11] Previous experiments[12-14] have demonstrated the splitting of the surface modes in thin films and have shown that the asymptotic energy is sensitive to very thin layers of contamination on the metal surfaces. However, the critical factor which determines the minimum observable value of k_s is the angular divergence of the incident beam; the apparatus described below has an angular resolution which is at least five times smaller than has been reported in other electron-energy-loss experiments.

Comparison of our results directly with theoretical predictions runs into difficulties arising from the lack of detailed information describing the composition, density, and dielectric constants of the natural oxide layer formed on aluminum by exposure to the atmosphere. Our approach to quantitative comparison is therefore in terms of the frequencies $\omega(k_s)$ which satisfy the dispersion relation for the metal-oxide system. A complete analysis would include the interaction probability of the incident fast electron with the normal surface modes of the system to give an intensity contour map[15] as a function of ω and k_s for a given angle of incidence. Although our intensity data behave qualitatively as expected, detailed measurements would be a useful test of the theory only in a metal-dielectric system where the various film thicknesses are controlled as independent parameters.[10,12,13] It is intended to make these measurements in the present apparatus, using evaporated dielectric films with well-known optical properties to protect the aluminum from oxidation. Experimental evidence for the existence of radiative surface plasmons inside the light lines has been considered elsewhere.[16]

II. EXPERIMENTAL

Polycrystalline aluminum films were prepared by electron-beam evaporation of high purity (99.999%) aluminum onto cleaved KCl substrates held at room temperature and also at liquid-

nitrogen temperature in an oil-free ultrahigh vacuum system. The background pressure was in the 10^{-8}-Torr range during evaporation. Growth rates (~10 Å sec^{-1}) and the total thickness of aluminum deposited were measured by a quartz-crystal monitor. Three film thicknesses (80, 160, and 320 Å) were chosen to cover the range where significant changes were expected in the surface-plasmon dispersion. Electron micrographs showed that the films were apparently smooth and continuous with a maximum grain size of about twice the film thickness, except in the case of the 80-Å films grown at room temperature. These films contained narrow discontinuities at the grain boundaries. The problem of smoothness and segregation of foreign atoms at boundaries is especially important because the plasmon wavelengths are comparable to the grain size. In particular, the theoretical curves are calculated for a smooth parallel-sided slab; there is evidence[17] that, for films grown under poor vacuum conditions, the presence of cracks and layers of oxide at the boundaries between grains is sufficient to change the dispersion relation. Additional evidence for this effect in the 80-Å films grown at room temperature is presented later, whereas the data obtained from a 80-Å film grown at liquid-N_2 temperature fit reasonably well. There is no such discrepancy for the thicker specimens. Unless otherwise noted, the following sections refer entirely to films which contain no visible discontinuities. However, all the films are inevitably oxidized on both surfaces during transfer to the electron spectrometer, because the film is floated off the substrate on water, mounted on a grid, and then examined in a light microscope to check for buckled areas. Total time of exposure to the atmosphere is about 15 min.

A Wien filter mounted below a conventional electron microscope[18] acts as a focusing spectrometer combined with a highly collimated source of high-energy electrons. The microscope is operated in the low-angle mode,[19] where the divergence of the beam at the specimen, using a pointed filament as an electron source, is 8×10^{-6} rad for 75-keV electrons. At an electron wavelength of 0.04 Å the corresponding precision, Δk_1, in k_1 is $k\Delta\theta \simeq 10^4$ cm^{-1}. Subsequent magnifying lenses increase the effective camera length of the system to 25 m at the entrance to the spectrometer. The Wien filter forms a focused dispersive image of the 150-μm-wide entrance slit which is then photographically recorded. The beam is positioned to pass exactly through the center of the slit so that the dispersed image forms a direct map of the intensity distribution as a function of $\hbar\omega$ and θ,

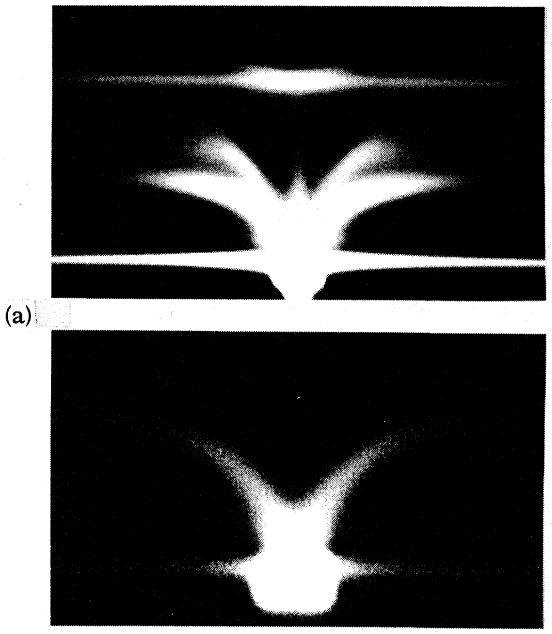

FIG. 1. Energy-loss spectra for transmission of 75-keV electrons through a 160-Å aluminum film at normal incidence; exposure times are 15 and 3 min. The energy axis is vertical and the horizontal lines correspond to volume plasmon excitation and to phonon and elastic scattering. The overexposed central spot contains electrons which undergo no elastic or inelastic collisions. A direct map of the surface-plasmon dispersion is formed. In Figs. 1-3 the lower picture is printed at 2 × relative magnification.

the electron energy loss and the angle of deflection (see Fig. 1). For normal incidence, θ is proportional to k_s. Spectra were also recorded for films tilted at a 60° angle about an axis perpendicular to the slit, corresponding to azimuthal angles ψ of 0° and 180° (see Figs. 2 and 3).[20] In this case, the parameters measured are $\hbar\omega$ and k_1 (see Fig. 4). Several plates with different exposure times were taken for each film because the variations in electron flux exceed the dynamic range of a single plate. The longest exposure time was 15 min.

In discussing our data, it is necessary to draw a distinction between the energy resolution as such and the precision with which the energy-loss value at the peak can be determined. Provided that the energy spread of the incident beam is symmetric, as it is under conditions of operation, and that there are no significant neighboring peaks, then the effect of the incident-beam energy spread is to broaden the peak rather than shift it. Under these conditions, the precision with which we can measure an energy loss corresponding to a peak position is given by drift in the electronic circuitry over the time of exposure and our ability to

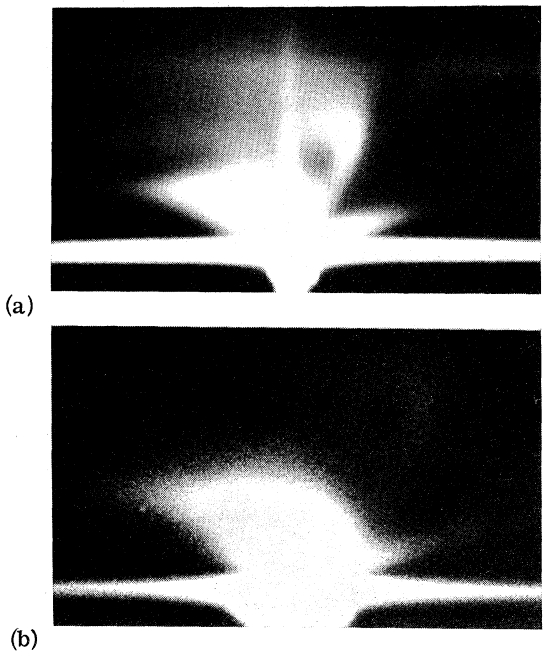

FIG. 2. Spectra for a 160-Å aluminum film recorded under the same conditions as in Fig. 1, except that the film is tilted at 60° to the beam. The surface-plasmon dispersion is transferred to a new coordinate system and the relative intensity of the ω^+ mode increases for $\psi = 180°$.

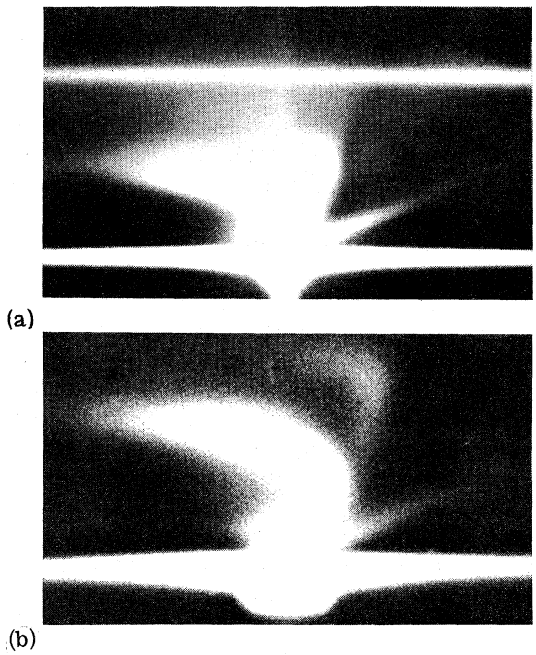

FIG. 3. Spectra for a 80-Å aluminum film tilted at 60° to the electron beam. Note that relative to Fig. 2, the splitting of the modes has increased and that the ω^+ mode is heavily damped where it crosses the energy axis.

locate the peak with the densitometer. These factors enable us to determine the position of peaks with a precision of ~0.1 eV. The position of the volume plasmon is used as an internal energy-calibration line for the system during microdensitometry of the plates. It can be shown that the change in the energy of the volume plasmon is insignificant over the range of the angles considered here. The error due to the nonlinearity of the energy axis[18] is ~1% over a range of 15 eV. We have assumed a volume-plasmon energy of 14.9 eV in agreement with the figure quoted by Festenberg[11] for aluminum films. A value of 14.95 ± 0.04 eV for a high-purity aluminum foil was obtained on the present apparatus, using a computer-linked scanning system.

The energy resolution—that is, the precision with which one can distinguish neighboring peaks—is limited primarily by the spread of energies in the incident beam. This becomes a significant factor in determining the widths of peaks. For any spectrum, a value for the effective energy resolution s can be found by measuring the half-width of the zero-loss line which contains both elastically and phonon-scattered electrons and is typically 0.7 eV. The plasmon widths w quoted below are deconvoluted values obtained from the formula $w = (w_m^2 - s^2)^{1/2}$, where w_m is the measured width.

A diffraction-grating replica is used to calibrate the angle of deflection, θ. In practice, the angular resolution may not reach 8×10^{-6} rad at angles very close to the undeviated beam, because the tail of the intensity distribution from the main

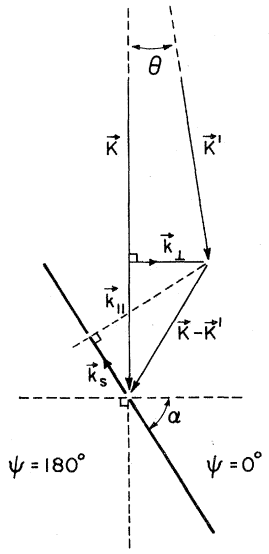

FIG. 4. Schematic diagram of the vector relationships for excitation of a surface plasmon in a tilted film. The magnitudes of the vectors are chosen to illustrate the case where the dispersion curves cross the energy axis; i.e., as $k_\perp$ increases, the sign of k_s is reversed. The change in momentum of the transmitted electron is given by $\vec{k}-\vec{k}'$.

beam is sufficient to swamp weak energy-loss peaks close to the origin. The vertical streak up the energy axis in Figs. 1 and 3 is due to scattering of the undeviated beam from the edge of the slit.

III. COMPARISON WITH THEORY

A. General background

The condition that nontrivial solutions exist for the fields defined by the Maxwell equations for charge oscillations at the surface of a metal slab, with thickness $2a$ surrounded by dielectric layers of equal thickness t on either side, can be expressed as an intrinsic equation relating $\omega_\pm$ and k_s,[13] such that

$$L^+ = \alpha_2\epsilon + \alpha_3\eta\,\frac{1-\nu e^{-2\alpha_2 t}}{1+\nu e^{-2\alpha_2 t}}\,\tanh(\alpha_3 a) = 0\ ,$$
$$L^- = \alpha_2\epsilon + \alpha_3\eta\,\frac{1-\nu e^{-2\alpha_2 t}}{1+\nu e^{-2\alpha_2 t}}\,\coth(\alpha_3 a) = 0\ , \qquad (1)$$

where ϵ and η are the complex dielectric constants of the metal and oxide layers, respectively, and $\nu = (\alpha_1\eta - \alpha_2)/(\alpha_1\eta + \alpha_2)$. The variation of the electric field with distance in the direction of the z axis, perpendicular to the plane of the slab, is controlled by $\alpha_1 = (k_s^2 - \omega^2/c^2)^{1/2}$, $\alpha_2 = (k_s^2 - \eta\omega^2/c^2)^{1/2}$, and $\alpha_3 = (k_s^2 - \epsilon\omega/c^2)^{1/2}$, which refer to the vacuum, dielectric, and metal, respectively. (The dielectric constant of the vacuum has been set equal to unity.) These solutions are obtained by imposing the requirement that the fields decay to zero as z tends to $\pm\infty$, where the origin is taken at the center of the slab. For complex ϵ and η, Eqs. (1) have no exact solution for real ω and k_s. Fuchs and Kliewer[21] have used a complex frequency, $\omega_1 + i\omega_2$, to find exact solutions for the secular equation, where $2\omega_2$ is a measure of the excitation width. This approach requires that the dielectric constants be accurately represented in an analytical form which satisfies the Kramers-Kronig relations, because ϵ and η are functions of a complex ω. For an unoxidized aluminum film in the long-wavelength limit, it is a reasonable approximation to use for ϵ the form for a damped free-electron gas. However, for most materials, the dielectric constants (measured as a function of a real ω) are far more complicated than this. Also, the use of a single parameter ω_2 to describe the width implies that the peak is symmetric; i.e., it is assumed that the dielectric constants do not vary much over the range $\omega_1 \pm \omega_2$. This is certainly not true close to a sharp absorption edge.

An alternative approach, which is used here, is to find the location of the maxima in the functions $\mathrm{Im}(-1/L^+)$, $\mathrm{Im}(-1/L^-)$ when calculated for a real ω. Because the complete expression[15] for the scattering of relativistic electrons from a single-layer film contains the parameters L^+ and L^- in the denominator of the various surface terms, a minimum in $|L^+|$ or $|L^-|$ leads to a peak in the intensity distribution. Provided that the peaks are narrow and reasonably symmetric, and there is no overlap between the ω^+ and ω^- peaks, the dispersion curves calculated in this way should accurately represent the locations of the maxima in the $\omega - k_s$ plane for electrons scattered by surface excitations.

B. Choice of dielectric constants

In making these calculations, the choice of dielectric constants becomes important. We first note that the standard form for a damped free-electron gas, $\epsilon = 1 - \omega_p^2/\omega(\omega - i\gamma)$,[20] is a relatively good representation of the dielectric constant for aluminum. Here ω_p is a volume-plasmon frequency in the absence of damping and γ is a phenomenological term independent of frequency. A variation in $\gamma(\omega)$ of approximately 50% has been detected optically but, since γ is about 5% of ω_p, this is still quite small.[22] On the other hand, typical oxide data (e.g., Arakawa and Williams[23]) indicate much more dramatic changes from the common assumption that $\epsilon_1 = 4.00$ and $\epsilon_2 = 0$. We are concerned with measurements spanning the range from 2 to 11 eV, in which ϵ_1 can show variations from 3.1 to 6.2 and ϵ_2 can range from 0 to 3.2. It therefore seems mandatory that we use the actual measurements for the oxide, but use of the standard form for the metal (which reduces the labor of computation significantly) is permissible. In our judgment this is compatible with the quality of our experimental measurements.

We plot the data not only in terms of the energy loss and scattering vector, but also in terms of dimensionless parameters r and q where $r = \omega/\omega_p$ and $q = ck_s/\omega_p$. The intrinsic damping term is approximated by the deconvoluted width of the volume plasmon. The values used in calculations are 0.75 eV for the 320- and 160-Å films and 1.3 eV for the 80-Å film, where the grain sizes are significantly smaller. These values agree with the range of energies quoted by Festenberg,[11] who finds a lower limit of 0.53 eV at small scattering angles for grain sizes larger than 250 Å.

For $q > 1$, the form of the dispersion curves is very sensitive to the thickness and dielectric constant of the oxide layers. In particular, the asymptotic energy $\hbar\omega_s$ is given by $\epsilon = -\eta$. The experimentally measured value of 6.7 eV, which agrees with previous measurements, implies that $\mathrm{Re}(\eta) \approx 4.0$ at this energy, provided we assume a

free-electron model for the metal with a small damping term. There are two sets of optical data available for the various forms of aluminum oxide. Measurements by Arakawa and Williams[23] on single-crystal α-alumina (corundum) extend from 5 to 28 eV. Below 8 eV, η_2 is zero and then rises rapidly to a peak value of 5 at 13 eV, whereas η_1 rises from 3.4 at 5 eV to a peak value of 6.2 at 9 eV. Using these experimental values the calculated asymptotic energy for the surface plasmon matches our experimental value (6.7 eV) exactly. The width is determined by the intrinsic damping in the metal, since $\eta_2 \approx 0$ at this energy.

The other set of data refers to anodized films (amorphous Al_2O_3) in the energy range 6.2–10.33 eV.[10] Here η_2 becomes nonzero at a lower energy (7.0 eV) while η_1 decreases from 3.61 at 6.89 eV to 1.92 at 10.33 eV. The curves are extrapolated to match values calculated from the optical data of Freeman[24] for anodized films between 12 and 25 eV. Below 5 eV, the data of Hass[25] for anodized films were used in all calculations, assuming $\eta_2 = 0$. In this energy range, the ω^+ and ω^- dispersion curves are less sensitive to η_1 and η_2, relative to the scatter in our data. Using these experimental values, the calculated asymptotic energy of 6.94 eV is somewhat higher than the measured value. However, a small upward adjustment of η_1 would be enough to give exact agreement.

The main point of interest lies in the behavior of the ω^+ curve as a function of η_1 and η_2. In all cases, we have also calculated the dispersion curves for $\eta_1 = 4$ and $\eta_2 = 0$ independent of frequency for the sake of comparison with the theoretical curves of Kloos[13] calculated on this basis. However, for the sake of clarity, we have not shown these curves on the diagrams and just note here that they lie between the two curves calculated for the two sets of physical data. Since $\eta_1 > 4$ for anodized films in the energy range 7–12 eV, this is expected. A somewhat more striking difference is that the peak widths show a steep rise when η_2 is nonzero, whereas with $\eta_2 = 0$ independent of frequency the limiting value is γ—the intrinsic damping in the metal.

Characteristic energy-loss data for anodized aluminum films and polycrystalline γ-alumina formed by heating aluminum films in air at 700 °C are available from the work of Swanson.[26] He finds the plasma resonance at 24.3 eV in γ-Al_2O_3 and at 22.6 eV in the lower-density amorphous film; the peak value of $\mathrm{Im}(-1/\epsilon)$ calculated from the dielectric constants for anodized films[24] is at 23.0 eV, whereas the optical data[23] for α-Al_2O_3 give a peak position at 25.7 eV. Also, there is a weak energy-loss peak at 8.7 eV in γ-Al_2O_3 which may correspond to the sharp absorption edge in α-Al_2O_3 above 8 eV. In the present experiments, no energy-loss structure definitely associated with the oxide layers alone is seen. No peak at 24 eV due to the plasmon loss in the oxide is visible. However, the loss is very broad[26] (9 eV) and there is considerable intensity in this region due to double scattering from the volume and surface plasmons in the aluminum. We conclude from these observations that the nature of the natural oxide layer on aluminum is not well characterized. Among other factors, the density variations and the presence or absence of water in the preparation process could be significant.

In principle, the thickness of the aluminum and oxide layers can be treated as independent parameters when fitting dispersion curves to the data, provided accurate figures are available for the optical properties of both the metal and dielectric. Then, an increase in the oxide thickness decreases the energy of both ω^+ and ω^- curves, while an increase in the aluminum thickness reduces the splitting of the two modes. The fitting procedure followed in the present case is described in Sec. IV.

The dispersion curves for tilted films are obtained by a simple geometrical transformation relating k_s and $k_\perp$ for a given energy,[27]

$$k_s = k_\perp \cos\alpha + (\omega/v)\sin\alpha \,, \tag{2}$$

where α is the angle of tilt, v is the velocity of the incident electron, and ω/v is equal to $k_\parallel$ (see Fig. 4). The line corresponding to zero k_s is given by $k_\perp = k_\parallel \tan\alpha$. Since the values of α calculated by averaging the data points are all within 2° of the nominal 60° tilt, the theoretical curves have been calculated for $\alpha = 60°$. Except in the region close to the energy axis, the scale of k_s is expanded for oblique incidence. The accuracy of measurements very close to the origin is limited by the presence of a peak at 1.5 eV due to an interband transition,[28,29] rather than by the resolution of the apparatus.

IV. DISCUSSION

Because the dispersion curves and peak widths are sensitive to variations in η, it is difficult to decide on a consistent scheme for comparing the data with theory. Primarily, changes in η_1 affect $\omega(k_s)$ while changes in η_2 affect the peak widths.[30] One important parameter for which there is no definite information is the conversion factor c, which defines the thickness of aluminum oxide formed from aluminum during natural oxidation; i.e., for an original thickness d Å of aluminum, if a layer of oxide t Å thick is formed on each side, the thickness of the remaining aluminum is

$2a = d - 2t/c$. The only parameter under experimental control is d, the thickness measured during deposition of the film. Typical values for c can be calculated from the molecular weights and densities for various forms of the oxide: (i) for γ-Al_2O_3, $c = 1.38$[26]; (ii) for amorphous Al_2O_3, $c = 1.82$[26]; (iii) for $Al_2O_3 \cdot H_2O$, $c = 2.0$[31]; (iv) for $Al_2O_3 \cdot 3H_2O$, $c = 3.2$.[31] There is evidence from inelastic electron tunneling measurements[32] that the natural oxide layer almost certainly exists in a hydrated form. For simplicity, a value for c of 2.0 is assumed in the following discussion and the effects of the two different choices for η are examined. Finally, another variable which is not considered here is that the two oxide layers may be of unequal thickness. Steinmann and Wille[33] have suggested that discrepancies in the intensity of optical emission curves may be due to a somewhat thicker layer of oxide on the side of the film which is floated off on water.

The ω^- curves are almost identical for a given a and t, except for the difference in the asymptotic energies, because the same optical data[25] are used below 5 eV. For the 160-Å film, a good fit is obtained for $t = 40$ Å and $2a = 120$ Å, taking $c = 2$ (Fig. 5). Likewise, for the 80-Å film, the corresponding figures are $t = 35$ Å and $2a = 45$ Å (Fig. 6). These thicknesses are similar to the range of 30–40 Å found by optical measurements,[34] and are consistent with the 50-Å thickness calculated by Cowan and Arakawa[9] for the natural oxide layer on an aluminum grating, using the amorphous data for η. An independent measure of the oxide thickness can be obtained from the 320-Å film because the dispersion is insensitive to changes in the aluminum thickness. In Fig. 7, the calculated curves are for $t = 40$ Å and $2a = 280$ Å.

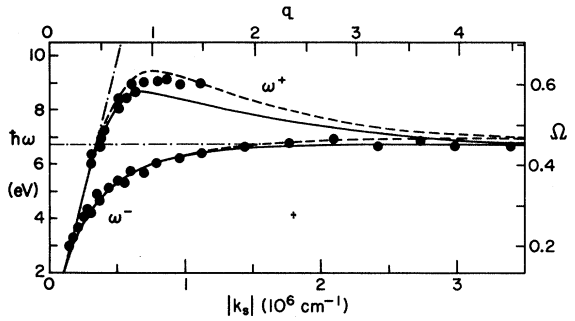

FIG. 5. Normal-incidence data for an aluminum film with a nominal thickness of 160 Å; the theoretical curves are calculated for $2a = 120$ Å, $t = 40$ Å, and $\gamma = 0.75$ eV. The dashed curves refer to η for amorphous aluminum oxide and the continuous curves to η for α- Al_2O_3. Typical error bars corresponding to $\Delta E = 0.1$ eV and $\Delta k_1 = 10^4$ cm^{-1} are included in Figs. 5–9.

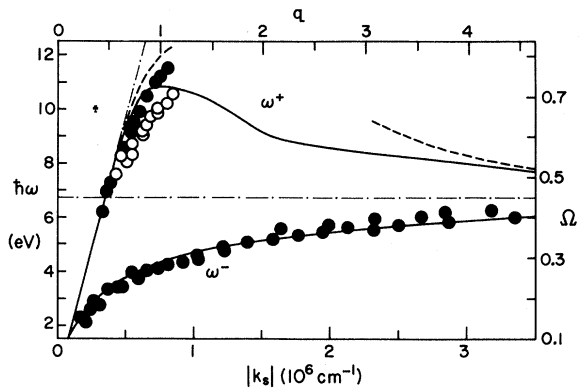

FIG. 6. Normal-incidence data for an aluminum film with a nominal thickness of 80 Å; the theoretical curves are calculated for $2a = 45$ Å, $t = 35$ Å, and $\gamma = 1.3$ eV. The open circles represent data for the ω^+ mode measured from a 80-Å film grown at room temperature which contains slight discontinuities (the ω^- mode is unchanged). The break in the ω^+ curve for the amorphous oxide indicates that there is no well-defined peak in $\mathrm{Im}(-1/L^+)$ over this range of k_s (see also Fig. 9). The dashed curves refer to η for amorphous aluminum oxide and the continuous curves to η for $\alpha - Al_2O_3$.

However, the error in t is certainly ±10 Å because there are several ambiguities in the data: (a) It is not clear that the measured peak positions for $q \sim 1$ correspond to either the ω^+ or ω^- curves because the splitting of the modes is at most 0.7 eV and the peak widths are larger than this;

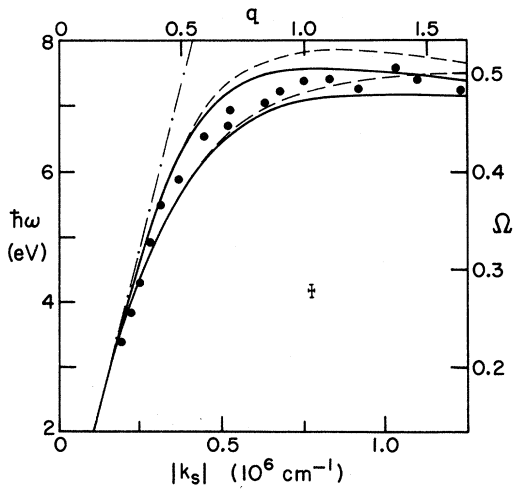

FIG. 7. Comparison of dispersion data for the 320-Å aluminum film at normal incidence with theoretical curves calculated for $2a = 280$ Å, $t = 40$ Å, and $\gamma = 0.75$ eV. Experimentally, the splitting of the modes is visible as an increase in the width, but it is not possible to measure the separate curves. The dashed curves refer to η for amorphous aluminum oxide and the continuous curves to η for α- Al_2O_3.

(b) there is a small but significant difference between the curves for the two forms of η. As in all the films, the asymptotic energy for large q is ~6.7 eV.

When the ω^+ dispersion curves for the 160- and 80-Å films are calculated using the values of a and t quoted above, it is found that the peak energies lie between the two theoretical curves (Figs. 5 and 6). A more rigorous test is given by comparison with the data for tilted films. For the 160-Å film (Fig. 8), the ω^- data are still a good fit to the tilted curves. Also, the ω^+ curves bracket the data over the entire range of $k_\perp$ for $\hbar\omega = 7.5$ eV and $k_\perp = -3.5\times10^6$ cm^{-1}. The 80-Å film, which contains the largest fraction of aluminum oxide, is most sensitive to the form of η. In fact, the ω^+ excitation is heavily damped for -1×10^6 cm$^{-1} < k_\perp < 0$ and appears to merge into the background intensity (Figs. 3 and 9). Likewise, the curves calculated from $\mathrm{Im}(-1/L^+)$ for the amorphous oxide increase monotonically from 0 to 14 eV for 0.8×10^6 cm$^{-1} < k_s < 2.4\times10^6$ cm^{-1}. The dispersion curves are not well defined in this range of k_s.

The corresponding ω^+ curve for α-Al_2O_3 has a sharp kink at 9 eV where γ_2 is changing rapidly. In general, the ω^+ peaks become wider and asymmetric at or above the absorption edge in the oxide, whereas the ω^- peaks always have widths which are less than or equal to γ. Over-all, the results are in reasonable agreement with theory. The data—particularly those presented in Fig. 9—suggest that the natural oxide is α-Al_2O_3. We would regard this as a tentative conclusion at this point, since we judge additional measurements on better-characterized samples necessary. Perhaps the most valuable conclusion is that judgments of this nature now appear to be feasible by this technique.

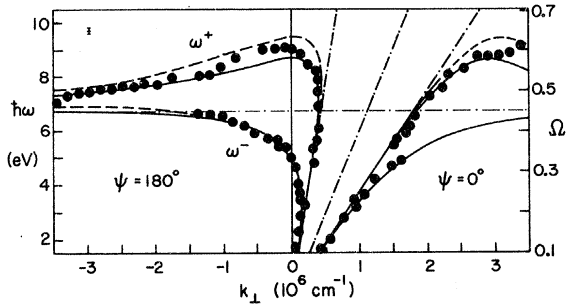

FIG. 8. Dispersion data for the 160-Å aluminum film tilted at 60°; the theoretical curves are calculated for the same parameters as in Fig. 5. The dashed curves refer to η for amorphous aluminum oxide and the continuous curves to η for α-Al_2O_3.

However, the dispersion data for 80-Å films grown at room temperature do not conform to this general conclusion. The measurements (Fig. 6) are limited to small values of k_s, but no dispersion curve calculated for any reasonable combination of aluminum and aluminum oxide thicknesses will fit the data. It is expected that the presence of discontinuities in the film on a scale comparable to the plasma wavelength will modify any dispersion relation calculated for planar layers. These results are supported by measurements[17] on aluminum films grown under poor vacuum conditions, where the observed dispersion curves are depressed in energy relative to the curves for films of the same thickness grown under cleaner conditions.

Theoretically, both ω^+ and ω^- peak widths decrease rapidly when close to the light line ($q < 1$), corresponding to the result derived by Fuchs and Kliewer[21] for an aluminum-vacuum interface, where the width ($2\omega_2$) is given by $q^2\gamma$ for $q \ll 1$. An equivalent calculation for a thin film shows that the width of the ω^+ mode decreases more rapidly than $q^2\gamma$, whereas the ω^- mode decreases more slowly. Experimentally, the measured widths are inaccurate, especially when close to the light line, where the angular divergence of the beam limits the resolution. Some approximate figures for peak widths at large k_s were found by subtracting the sloping background intensity. The width of the ω^- branch is close to the volume-plasmon width but is always 0.1–0.2 eV larger, possibly because η_2 is nonzero between 6 and 7 eV. The ω^+ branch is more heavily damped; measurements for large k_s taken from tilted films give widths ~2γ.

Finally, the intensity distribution for normal in-

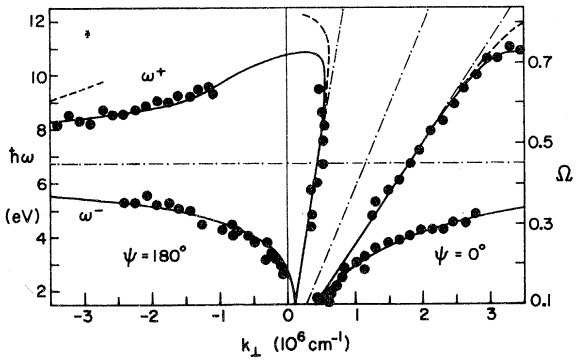

FIG. 9. Dispersion measurements for the 80-Å aluminum film tilted at 60°; the theoretical curves are calculated for the same parameters as in Fig. 6. For $\psi = 180$, the ω^+ mode merges into the background intensity above ~9.5 eV. The dashed curves refer to η for amorphous aluminum oxide and the continuous curves to η for α-Al_2O_3.

cidence is qualitatively similar to the contour map for a 100-Å clean film discussed by Kröger,[15] except for the change in the asymptotic energy. The ω^- branch shows a rapid decrease in intensity as k_s increases. The ω^+ branch is well defined relative to the background intensity only for values of k_s between 0.3×10^6 and 1.2×10^6 cm^{-1} (160-Å film) or 0.8×10^6 cm^{-1} (80-Å film).

The intensity distribution in tilted films is asymmetric, with higher intensities for $\psi=180°$.[3] In addition, the intensity of the ω^+ mode increases relative to the ω^- mode as predicted by Otto and Swan.[27] For $\psi=0°$ and 180°, there exist characteristic values for $|k_\perp|$ where the intensities of the ω^+ and ω^- modes are equal. Experimentally, these two wave numbers are almost identical; for the 160-Å film, $|k_\perp|=1.3-1.4\times10^6$ cm^{-1}, and for the 80-Å film, $|k_\perp|=1.85-1.95\times10^6$ cm^{-1}. Our results indicate that it is important to use the complete frequency-dependent dielectric constant when calculating dispersion curves for surface excitations, even for relatively thin layers of contamination.

---

*Work supported initially by the U.S. Atomic Energy Commission under Contract Nos. AT(30-1)-3156 and C00-3156-55, and completed through the Materials Science Center at Cornell University supported by the NSF under Grant No. GM 33637.

†Present address: Sandia Laboratories, Albuquerque, N.M. 87115.

[1]C. B. Duke and A. Bagchi, J. Vac. Sci. Technol. 9, 238 (1972).
[2]R. H. Ritchie, Phys. Rev. 106, 874 (1957).
[3]E. A. Stern and R. A. Ferrell, Phys. Rev. 120, 130 (1960).
[4]R. H. Ritchie and H. B. Eldridge, Phys. Rev. 126, 1935 (1962).
[5]A. Otto, Z. Phys. 185, 232 (1965).
[6]E. N. Economou, Phys. Rev. 182, 539 (1969).
[7]A. Otto, Phys. Status Solidi 26, K99 (1968).
[8]Ye-Yung Teng and E. A. Stern, Phys. Rev. Lett. 19, 511 (1967).
[9]J. J. Cowan and E. T. Arakawa, Z. Phys. 235, 97 (1970).
[10]J. J. Cowan and E. T. Arakawa, Phys. Status Solidi (a) 1, 695 (1970).
[11]C. V. Festenberg, Z. Phys. 207, 47 (1967).
[12]C. Kunz, Z. Phys. 196, 311 (1966).
[13]T. Kloos, Z. Phys. 208, 77 (1968).
[14]J. B. Swan, A. Otto, and H. Fellenzer, Phys. Status Solidi 23, 171 (1967).
[15]E. Kröger, Z. Phys. 216, 115 (1968).
[16]R. Vincent and J. Silcox, Phys. Rev. Lett. 31, 1487 (1973).
[17]R. B. Pettit and J. Silcox, J. Appl. Phys. 45, 2858 (1974).
[18]G. H. Curtis and J. Silcox, Rev. Sci. Instr. 42, 630 (1971). R. B. Pettit, J. Silcox, and R. Vincent, in *Proceedings of the 29th Electron Microscopy Society of America*, edited by C. J. Arcenaux (Claitors, Baton Rouge, Louisiana, 1971), p. 176. P. E. Batson, J. Silcox, and R. Vincent (unpublished).
[19]R. H. Wade and J. Silcox, Phys. Status Solidi 19, 57 (1967); 19, 63 (1967).
[20]See, for example, H. Raether, Springer Tracts Mod. Phys. 38, 85 (1965).
[21]R. Fuchs and K. L. Kliewer, Phys. Rev. B 3, 2270 (1970).
[22]W. R. Hunter, J. Opt. Soc. Am. 54, 208 (1964); R. C. Vehse, E. T. Arakawa, and J. L. Stanford, *ibid.* 57, 551 (1967).
[23]E. T. Arakawa and M. W. Williams, J. Phys. Chem. Solids 29, 735 (1967).
[24]G. H. C. Freeman, Brit. J. Appl. Phys. 16, 927 (1965).
[25]G. Hass, J. Opt. Soc. Am. 39, 532 (1949).
[26]N. Swanson, Phys. Rev. 165, 1067 (1967).
[27]A. Otto and J. B. Swan, Z. Phys. 206, 277 (1967).
[28]H. Ehrenreich, H. R. Philipp, and B. Segall, Phys. Rev. 132, 1918 (1962).
[29]A. Imbusch, Z. Phys. 216, 94 (1968).
[30]H. Raether, Surf. Sci. 8, 233 (1967).
[31]*Handbook of Chemistry and Physics, 51st ed.* (Chemical Rubber, Cleveland, Ohio, 1971), p. B-64.
[32]A. L. Geiger, B. S. Chandrasekhar, and J. G. Adler, Phys. Rev. 188, 1130 (1969).
[33]W. Steinmann and H. Wille, Phys. Status Solidi 15, 507 (1966).
[34]R. P. Madden, L. R. Canfield, and G. Hass, J. Opt. Soc. Am. 53, 620 (1963).

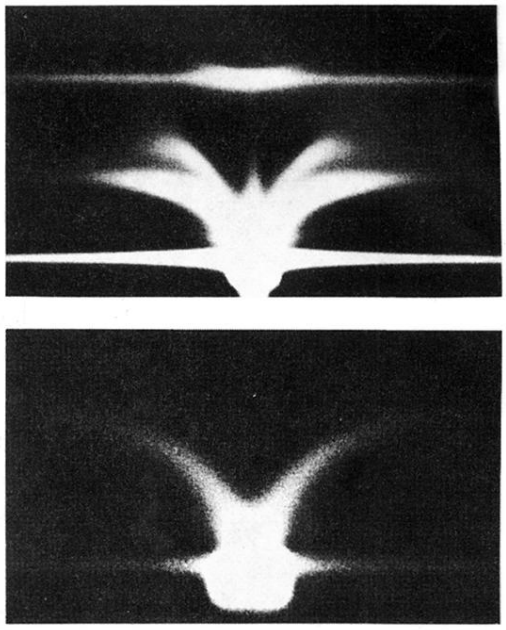

(a)

(b)

FIG. 1. Energy-loss spectra for transmission of 75-keV electrons through a 160-Å aluminum film at normal incidence; exposure times are 15 and 3 min. The energy axis is vertical and the horizontal lines correspond to volume plasmon excitation and to phonon and elastic scattering. The overexposed central spot contains electrons which undergo no elastic or inelastic collisions. A direct map of the surface-plasmon dispersion is formed. In Figs. 1-3 the lower picture is printed at 2 × relative magnification.

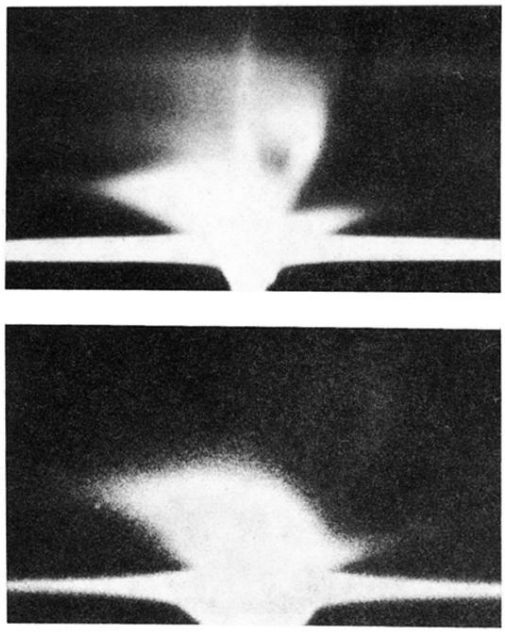

(a)

(b)

FIG. 2. Spectra for a 160-Å aluminum film recorded under the same conditions as in Fig. 1, except that the film is tilted at 60° to the beam. The surface-plasmon dispersion is transferred to a new coordinate system and the relative intensity of the ω^+ mode increases for $\psi = 180°$.

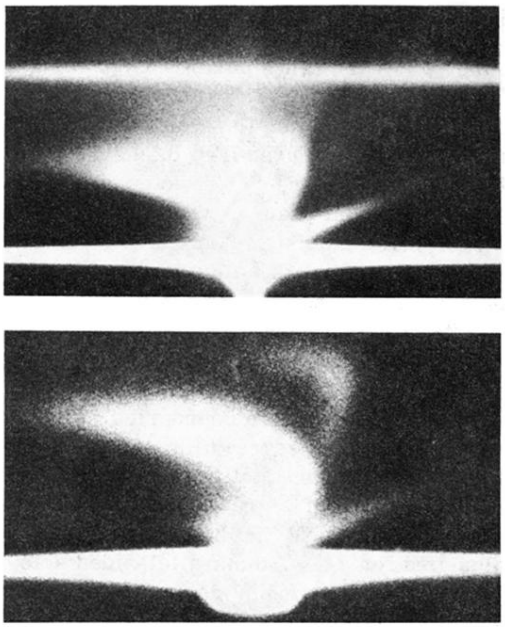

FIG. 3. Spectra for a 80-Å aluminum film tilted at 60° to the electron beam. Note that relative to Fig. 2, the splitting of the modes has increased and that the ω^+ mode is heavily damped where it crosses the energy axis.